

1 **Why is *Trichodesmium* abundant in the Kuroshio?**

2 T. Shiozaki^{1,2}, S. Takeda^{1,3}, S. Itoh², T. Kodama^{1,4}, X. Liu^{1,5}, F. Hashihama⁶, K.

3 Furuya¹

4 [1]{Department of Aquatic Bioscience, Graduate School of Agricultural and Life

5 Sciences, The University of Tokyo, Tokyo, 113-8657, Japan}

6 [2]{Atmosphere and Ocean Research Institute, The University of Tokyo, Chiba,

7 277-8564, Japan}

8 [3]{Faculty of Fisheries, Nagasaki University, Nagasaki, 852-8521, Japan}

9 [4]{Japan Sea National Fisheries Research Institute, Fisheries Research Agency,

10 Niigata, 951-8121, Japan}

11 [5]{College of Ocean and Earth Sciences, Xiamen University, Xiamen, 361005,

12 China}

13 [6]{Department of Ocean Sciences, Tokyo University of Marine Science and

14 Technology, Tokyo, 108-8477, Japan}

15

16 Corresponding to: T. Shiozaki (shiozaki@ori.u-tokyo.ac.jp)

17 **Abstract**

18 The genus *Trichodesmium* is recognized as an abundant and major diazotroph in the
19 Kuroshio, but the reason for this remains unclear. The present study investigated the
20 abundance of *Trichodesmium* spp. and nitrogen fixation together with concentrations
21 of dissolved iron and phosphate in the Kuroshio and its marginal seas. We performed
22 the observations near the Miyako Islands, which form part of the Ryukyu Islands,
23 situated along the Kuroshio, since our satellite analysis suggested that material
24 transport could occur from the islands to the Kuroshio. *Trichodesmium* spp. bloomed
25 ($>20,000$ filaments L^{-1}) near the Miyako Islands, abundance was high in the Kuroshio
26 and the Kuroshio bifurcation region of the East China Sea, but was low in the
27 Philippine Sea. The abundance of *Trichodesmium* spp. was significantly correlated
28 with the total nitrogen fixation activity. The surface concentrations of dissolved iron
29 (0.19–0.89 nM) and phosphate (<3–36 nM) were similar for all of the study areas,
30 indicating that the nutrient distribution could not explain the spatial differences in
31 *Trichodesmium* spp. abundance and nitrogen fixation. Numerical particle-tracking
32 experiments simulated the transportation of water around the Ryukyu Islands to the
33 Kuroshio. Our results indicate that *Trichodesmium* growing around the Ryukyu
34 Islands could be advected into the Kuroshio.

36 **1. Introduction**

37 The Kuroshio is a western boundary current in the North Pacific Ocean that
38 originates in the North Equatorial Current and bifurcates to the east of the Philippines.
39 The main stream of the Kuroshio enters the East China Sea (ECS) northeast of Taiwan,
40 flows out through the Tokara Strait, and runs along the Japanese islands of Shikoku
41 and Honshu. While the Kuroshio and its adjacent waters are characterized by highly
42 oligotrophic conditions, phytoplankton and zooplankton communities in the Kuroshio
43 are distinct compared to those from adjacent waters (McGowan, 1971). McGowan
44 (1971) suggested that some plankton species are delivered by the Kuroshio to the
45 north from the equatorial region.

46 The abundance of the cyanobacterial genus *Trichodesmium* in the Kuroshio is
47 much higher than that in neighboring seas (Marumo and Asaoka, 1974). Because
48 *Trichodesmium* is a major nitrogen fixer in the Kuroshio, it is believed to be the key
49 genus for understanding the Kuroshio ecosystem (Chen et al., 2008, 2014; Shiozaki et
50 al., 2014a). Nevertheless, the factors controlling the distribution of *Trichodesmium* in
51 this region are poorly understood. Marine nitrogen fixation is thought to be regulated
52 by the supply of iron and phosphorus (Mahaffey et al., 2005), and *Trichodesmium*
53 thrives in iron-rich oligotrophic regions (Moore et al., 2009; Shiozaki et al., 2010,

54 2014b). A major source of iron in the ocean is atmospheric dust deposition (Jickells et
55 al., 2005; Mahowald et al., 2009). Modeling studies indicate that dust deposition in
56 the western North Pacific decreases exponentially from the continental shelf to the
57 Philippine Sea (Jickells et al., 2005; Mahowald et al., 2009), and hence, deposition is
58 not as high in the Kuroshio as in the adjacent waters. As for phosphorus limitation,
59 iron-enhanced nitrogen fixation causes phosphorus depletion, and the nitrogen
60 fixation is consequently limited by phosphorus (Mather et al., 2008). The phosphate
61 distribution has been examined in this study region using a conventional colorimetric
62 method, and the surface phosphate concentration in the Kuroshio has been reported to
63 be as low as that in the Philippine Sea (Chen, 2008). Therefore, the distinct high
64 abundance of *Trichodesmium* in the Kuroshio is probably not explained by nutrient
65 and trace metal concentrations; however, distributions of dissolved iron and phosphate
66 at the nanomolar level have not been well studied in this region (Obata et al., 1997;
67 Shiozaki et al., 2010; Kodama et al., 2011).

68 Nitrogen fixation by *Trichodesmium* has recently also been found to be active
69 around oceanic islands; New Caledonia Island, Efate Island, Fiji Island, Tahiti Island,
70 and Northern Mariana Islands (Shiozaki et al., 2010, 2013, 2014c; Lin et al., 2011).
71 Furthermore, these studies demonstrated that abundant *Trichodesmium* is delivered by

72 the current to areas that are remote from the islands. Although this phenomenon was
73 noted in the western Pacific warm pool and western South Pacific, it can also occur in
74 and around the Kuroshio and may contribute to the distribution of *Trichodesmium* in
75 this region.

76 In the present study, we simultaneously determined *Trichodesmium* abundance
77 and bulk water nitrogen fixation together with concentrations of dissolved iron and
78 phosphate at the nanomolar level in the Kuroshio and its marginal seas. In addition,
79 we conducted intensive observations around the Miyako Islands section of the
80 Ryukyu Islands located close to the main stream of the Kuroshio.

81

82 **2. Materials and Methods**

83 **2.1. Oceanographic database**

84 Algal blooms in an oligotrophic region may indicate a nitrogen fixation hotspot
85 (Wilson and Qiu, 2008; Shiozaki et al., 2014c). To identify the locations of intensive
86 algal blooms, we used a dataset of chlorophyll (chl) *a* observed by satellite. According
87 to Wilson and Qiu (2008), an algal bloom in an oligotrophic region can be defined as
88 a surface chl *a* value $>0.15 \text{ mg m}^{-3}$ in summer. In the present study, we used 8-day,
89 moderate-resolution imaging spectroradiometer (MODIS) Aqua level 3 chl *a* with 9

90 km resolution during summer between July 2003 and September 2009. We defined
91 summer as July through September. The bloom frequency for each pixel was
92 calculated from the ratio of counts in which chl *a* was $>0.15 \text{ mg m}^{-3}$ to the total
93 counts in which chl *a* was detected.

94 To examine the current field, geoelectrokinetograph and ship-mounted acoustic
95 Doppler current profiler (ADCP) data from the uppermost layer for the summers
96 between 1953 and 2008 were obtained from the Japan Oceanographic Data Center
97 (<http://www.jodc.go.jp>). Regridding, removal of anomalous values, and smoothing of
98 the dataset were performed as described by Isobe (2008).

99

100 2.2. Cruise observations

101 Experiments were conducted during summer on-board the R/V *Tansei-maru*
102 (KT-06-21, September 9–17, 2006; KT-07-22, September 5–13, 2007; KT-09-17,
103 September 8–13, 2009; KT-10-19, September 4–12, 2010) and the T/V
104 *Nagasaki-maru* (242, July 19–28, 2007) (Fig. 1a, Table S1). The stations during the
105 KT-06-21, KT-07-22, and *Nagasaki-maru* 242 cruises were divided into three areas
106 based on the temperature-salinity diagram (see Fig.2 of Shiozaki et al., 2011): the
107 ECS, Kuroshio, and Philippine Sea. During the KT-09-17 cruise, we conducted

108 experiments around the Miyako Islands which were distinguished from the other three
109 areas. During the KT-10-19 cruise, we performed observations in the ECS, the
110 Kuroshio, and around the Miyako Islands (Liu et al., 2013).

111

112 2.2.1. Light intensity, hydrography, nutrients, and chl a

113 Water samples for all of the experiments, with the exception of determination of
114 the dissolved iron concentration, were collected using an acid-cleaned bucket and
115 Niskin-X bottles. The depth profile of light intensity was determined immediately
116 before the water sampling using a light sensor (during the KT-06-22, KT-07-21,
117 KT-09-17, and KT-10-19 cruises) or an empirical equation (during the *Nagasaki-maru*
118 242 cruise) (Shiozaki et al., 2011). Temperature and salinity profiles to a depth of 200
119 m were obtained using a conductivity, temperature, and depth (CTD) sensor. Mixed
120 layer depth (MLD) was defined as the depth at which the σ_t increased by 0.125
121 from its value at a depth of 10 m. Water samples for nitrate+nitrite (N+N) and
122 phosphate were collected from 0, 10, 30, 40, 50, 60, 70, 80, 90, 100, 125, 150, and
123 200 m, and from depths at given light intensities. At all of the stations, the N+N and
124 phosphate concentrations were determined at the nanomolar level using a
125 supersensitive colorimetric system consisting of an AutoAnalyzer II (Technicon) and

126 Liquid Waveguide Capillary Cells (World Precision Instruments, USA) (Hashihama et
127 al., 2009). The detection limits of N+N and phosphate were both 3 nM. When the
128 concentration was greater than 0.1 μ M, it was determined by conventional methods
129 using a TRAACS 2000 autoanalyzer (Bran:Luebbe, UK). In addition to the
130 observations at the stations, temperature, salinity, and the *in vivo* chl fluorescence of
131 the surface water were monitored continuously during the cruises by a
132 thermosalinograph (Ocean Seven, Idronaut, Italy) and a fluorometer (Minitracka,
133 Chelsea, UK).

134

135 2.2.2. Dissolved iron

136 Water was sampled to estimate the dissolved iron concentration from 0.5-m depth
137 during the KT-06-21 and KT-07-22 cruises and from 10-m depth during the KT-09-17
138 cruise using an acid-cleaned Teflon bellows pump (AstiPure PFD2; Saint-Gobain)
139 with Teflon tubing (inner diameter = 12 mm). The water was filtered through an
140 acid-cleaned 0.22 μ m pore filter (Millipak100; Millipore) connected to the in-line of
141 the Teflon tubing with a Teflon connector. Filtered seawater was collected in a 125
142 mL low-density polyethylene (LDPE) bottle (Nalgene, Nalge Nunc International),
143 which had been washed using following technique: the sample bottles were

144 sequentially cleaned by soaking in 5% alkali detergent for at least 2 days, in 4 N HCl
145 for at least 1 day, in 0.3 N metal analysis-grade HNO₃ at 60°C overnight, and finally,
146 in Milli-Q water at 60°C overnight. After rinsing with Milli-Q water, the bottles were
147 dried in a laminar flow space and stored in double plastic bags. The filtrate samples
148 were acidified to a pH <1.7 with trace-metal-grade HCl (Tamapure AA-100; Tama
149 Chemicals) in a Class-100 clean-air bench, and stored at room temperature for more
150 than 1 year.

151 The dissolved iron concentration was determined using an automatic Fe(III) flow
152 injection analytical system (Kimoto Electric Co., Ltd.) using a chelating resin
153 pre-concentration and chemiluminescence detection method (Obata et al., 1993). A
154 buffer solution of 10 M formic acid and 2.4 M ammonium formate was added to the
155 samples. The sample pH was adjusted to 3.0 with 20% ammonium hydroxide
156 (NH₄OH; Tamapure AA-10; Tama Chemicals) immediately prior to analysis. The
157 detection limit of this method was 0.05 nM. The SAFe reference standards S1 and D2
158 were measured during the course of sample analysis, and the results were within the
159 range of the published consensus values: S1 = 0.097 ± 0.043 nM and D2 = 0.91 ±
160 0.17 nM (Johnson et al., 2007).

161

162 **2.2.3. Nitrogen fixation and abundance of *Trichodesmium* spp.**

163 Samples for the incubation experiments were collected vertically at all of the
164 stations, except at Sts. T0621, GN-3, and T0905, where samples were only collected
165 from the surface. All samples were collected in duplicate in acid-cleaned 4.5-L
166 polycarbonate bottles. During the *Nagasaki-maru* 242 cruise, water samples were
167 collected from four different depths corresponding to 100%, 25%, 10%, and 1% of the
168 surface light intensity. During the other cruises, samples were collected from a depth
169 of 50% surface light intensity. Samples at 100% surface light intensity were collected
170 from 0 m during all of the cruises, except during the KT-10-19 cruise in which the
171 samples were collected from a depth of 5 m. The bulk water nitrogen fixation activity
172 was determined based on primary production using a dual isotopic ($^{15}\text{N}_2$ and ^{13}C)
173 technique (Shiozaki et al., 2009). After ^{13}C -labeled sodium bicarbonate (99 atom%
174 ^{13}C ; Cambridge Isotope Laboratories) was added to each bottle, 2 mL of $^{15}\text{N}_2$ gas (98
175 atom% ^{15}N ; SI Science Co. Japan) was injected directly into the incubation bottles
176 through a septum using a gastight syringe. The bottles were covered with
177 neutral-density screens to adjust the light level and incubated for 24 h in an on-deck
178 incubator cooled by flowing surface seawater for 24 h. We determined the nitrogen
179 fixation activity using the $^{15}\text{N}_2$ gas bubble addition method (Montoya et al., 1996).

180 This method is believed to underestimate the nitrogen fixation rate relative to the $^{15}\text{N}_2$
181 gas dissolution method (Mohr et al., 2010). The start time of incubation in this study
182 varied at each station (Table S1). Considering daily periodicity of nitrogen fixation in
183 each diazotroph (Zehr, 2011) and the time to reach equilibration of the $^{15}\text{N}_2$ gas
184 bubble with seawater (>12 h, Mohr et al., 2010), the level of underestimation could
185 vary at each station. Meanwhile, the level of underestimation is thought to be low in
186 *Trichodesmium* dominant water because *Trichodesmium* can float to the top of the
187 bottle and directly use the added $^{15}\text{N}_2$ in the bubble method (Großkopf et al., 2012).
188 Although the bias of underestimation could not be estimated from the results in this
189 study, the actual nitrogen fixation rate could be higher than the obtained rate.

190 A recent study demonstrated that commercial $^{15}\text{N}_2$ gas could be contaminated by
191 ^{15}N -labeled nitrate and ammonium (Dabundo et al., 2014). We tested the
192 contamination in $^{15}\text{N}_2$ gas produced by SI Science Co., Ltd., which was used (from
193 different batch numbers) in the present study (see Supporting Information). Briefly,
194 the $^{15}\text{N}_2$ gas was dissolved in aged subtropical surface water, and concentrations of
195 nitrate, nitrite, and ammonium at the nanomolar levels were determined using
196 supersensitive colorimetric systems. The results showed that there were no significant
197 differences between the control and samples to which $^{15}\text{N}_2$ had been added (Fig. S1),

198 suggesting that the contamination of nitrate, nitrite, and ammonium in the $^{15}\text{N}_2$ gas
199 was insignificant (Supporting Information).

200 Water samples were collected for microscopic analysis at all light depths during
201 the *Nagasaki-maru* 242 and KT-07-21 cruises, and only from the surface during the
202 KT-06-22, KT-09-17, and KT-10-19 cruises. The samples were fixed using acidified
203 Lugol's solution. *Trichodesmium* spp. were counted using the Utermöhl method under
204 inverted microscope observation. *Trichodesmium* greater than ca. 300 μm in length
205 were counted as 1 filament and shorter lengths were counted as 0.5 filaments. In
206 addition, phytoplankton other than *Trichodesmium* spp. were identified from the
207 samples obtained during the KT-09-17 cruise.

208

209 2.3. Statistical analysis of environmental variables

210 We used non-metric multi-dimensional scaling (nMDS) to investigate the spatial
211 differences in the environmental variables that could influence *Trichodesmium* growth
212 and bulk water nitrogen fixation; temperature, mixed layer depth, nitrate, dissolved
213 iron, and phosphate. The environmental variables were transformed by $\log_{10}(x + 1)$
214 prior to analysis. A dissimilarity/similarity matrix between stations was constructed
215 using the Bray-Curtis index. The nMDS was used to visualize similarities in the

216 environmental variables among the stations. An Analysis of Similarity (ANOSIM)
217 was used to test the differences in the environmental variables among the stations.
218 The nMDS and ANOSIM analyses were performed using PRIMER 6 software.

219

220 2.4. Numerical experiments

221 Numerical particle-tracking experiments were conducted to investigate the
222 transport of water masses at the surface from areas around the Miyako Islands in the
223 summer season from 2003 to 2009. Surface velocity data were derived from the
224 FRA-JCOPE2 reanalysis product (Miyazawa et al., 2009), which is an eddy-resolving
225 ($1/12^\circ$) ocean model combined with three-dimensional variational data assimilation
226 (satellites, ARGO floats, and shipboard observations), and is one of the most reliable
227 models for the region around Japan for the above time period. The method of tracking
228 particles was basically the same as in Itoh et al. (2009), but we did not include the
229 random walk for simplicity. The release points of particles were selected at the surface
230 of the model grid points around the coastal waters of the Miyako Islands. We assumed
231 that the particles did not increase, die, or sink from the surface during the experiments.
232 To focus on transport during the summer season (July–September), particles were
233 released one month before the summer (June 1) and were tracked until September 30.

234 To examine differences in the output depending on the start time within the same
235 year, we also performed experiments starting on June 1, 11, and 21, and July 1 in
236 2009. The ratio of particles that reached areas downstream of the Tokara Strait
237 (hereafter Area K) (Fig. 7), including the particles' entrainment to the Kuroshio, to
238 total particles released from the Miyako Islands was computed in all experiments. It
239 should be noted that these experiments contained the following two uncertainties.
240 First, the distribution of *Trichodesmium* around the islands, which strongly influences
241 the destinations of particles, was not able to be determined in advance.
242 *Trichodesmium* is known to aggregate and not to occur uniformly in the ocean
243 (Capone et al., 1997). Second, the model cannot reproduce the current very close to
244 the islands. If a water mass very near the islands was delivered to the open ocean by
245 tide and/or river plumes that were not considered in the model, seaward dispersion of
246 particles was likely underestimated.

247

248 **3. RESULTS**

249 **3.1. The Kuroshio path and bloom frequency**

250 The average surface current field indicated that the main stream of the Kuroshio
251 flowed along the continental shelf in the ECS, and then passed to the south of the

252 Kyushu and Shikoku Islands (Fig. 1b). In addition, the Kuroshio branch bifurcated
253 northward at 25°N and 30°N at the continental shelf. Hence, all of the stations in the
254 ECS were subject to the influence of the Kuroshio. While the northeastward stream of
255 the Kuroshio was prominent in this region, smaller-scale flows and circulations were
256 observed in the areas around and to the southeast of the Ryukyu Islands. In the west of
257 the main stream of the Kuroshio, because the average chl *a* was over 0.15 mg m⁻³ (Fig.
258 S2), the frequency of chl *a* values >0.15 mg m⁻³ was high (Fig. 1b). In contrast, the
259 bloom frequency in the east of the main stream of the Kuroshio differed from the
260 distribution of the average chl *a*; algal blooms occurred frequently in the Ryukyu
261 Islands. Around the Miyako Islands, water of high bloom frequency was located to the
262 west of the islands, extending to the north.

263

264 3.2. Region-wide environmental conditions, *Trichodesmium* spp., and 265 nitrogen fixation

266 The sea surface temperature (SST) ranged from 25.1–30.5°C at all of the stations
267 (Table S1), and there were no significant differences among the areas ($p>0.05$,
268 Tukey's honestly significant difference [HSD] test). The MLD varied from 12–60 m
269 at all of the stations, and was relatively deep around the Miyako Islands compared to

270 the other areas (Table S1). The surface N+N concentration varied between <3 and 42
271 nM, except around the Miyako Islands (Shiozaki et al., 2010, 2011) (Table S1). The
272 highest surface N+N concentration (374 nM) was observed at St. T0904 where
273 upwelling occurred (see below). No significant difference in the surface N+N was
274 observed among the four areas ($p>0.05$, Tukey's HSD test). The surface phosphate
275 concentration varied between <3 and 36 nM at all of the stations (Fig. 2a). The
276 phosphate concentrations at the surface and within the MLD were not significantly
277 different among the four areas ($p>0.05$, Tukey's HSD test). There was a greater
278 increase in the phosphate concentrations below 40–50 m in the ECS compared to the
279 other areas (Fig. 3a–d). Furthermore, the phosphate concentrations below 40–50 m
280 near the Miyako Islands were higher than those in the Kuroshio and the Philippine
281 Sea, which were depleted down to 100 m, except at St. T1004 located near the
282 continental shelf. The N/P (= N+N/phosphate) ratio at the surface varied from 0.28 to
283 6.40 except at St. T0904 (N/P = 16.3) (Table S1), and no significant differences were
284 observed among the four areas ($p > 0.05$, Tukey's HSD test). The surface dissolved
285 iron concentration ranged from 0.19 to 0.89 nM at all of the stations (Fig 2b), with no
286 significant spatial differences among the four areas ($p>0.05$, Tukey's HSD test). The
287 surface dissolved iron concentrations at Sts. T0622 and T0907 were elevated to 0.83

288 nM and 0.89 nM, respectively, with lower salinity water than in the adjacent waters
289 (salinity data are shown in Fig. 4a and Kodama et al., 2011). The nMDS showed that
290 the environmental variables at all stations were the same at the >80% similarity level
291 and were >90 % similar excepting station T0904 (Fig. 5). The ANOSIM indicated no
292 significant differences among the stations ($p > 0.05$).

293 The abundance of *Trichodesmium* spp. was highest at the surface at almost all of
294 the stations during the *Nagasaki-maru* 242 and KT-07-21 cruises (Fig. S3). The
295 surface *Trichodesmium* spp. abundances were positively correlated with the
296 depth-integrated abundances ($r^2 = 0.51$, $p < 0.05$) (Fig. 6a). Thus, the surface
297 abundance was used to discuss the geographical distribution of *Trichodesmium* spp.
298 The *Trichodesmium* spp. abundance at the surface varied widely, and there was no
299 significant difference among the four areas ($p > 0.05$, Tukey's HSD test).
300 *Trichodesmium* spp. were observed at all of the stations in the Kuroshio and around
301 the Miyako Islands, whereas they were not always observed in the ECS and the
302 Philippine Sea (Fig. 2c). The average surface abundance in the Philippine Sea was the
303 lowest among all of the areas (Table 1). The highest abundance of *Trichodesmium* spp.
304 (>20000 filaments L⁻¹) was observed near the Miyako Islands at St. T0906, where
305 they bloomed (see below). Tuft-shaped colonies were found at Sts. T0706, T0723,

306 CK-10, and T0906. The nitrogen fixation rate was highest in the upper 25% light
307 depth, and decreased with increasing depth at all of the stations (Fig. 3e–h). The
308 surface rates were positively correlated with the depth-integrated rates ($r^2 = 0.79$, $p <$
309 0.05) (Fig. 6b), suggesting that the distribution of nitrogen fixation was indexed by
310 the surface activity. Surface and depth-integrated nitrogen fixation ranged from 0.54
311 to 62 $\text{nmol N L}^{-1} \text{d}^{-1}$ and from 29.5 to 753 $\mu\text{mol N m}^{-2} \text{d}^{-1}$, respectively (Fig. 2d and
312 Table S1). Surface nitrogen fixation in the Philippine Sea was significantly lower than
313 that in the Kuroshio ($p < 0.05$, t -test).

314 The surface abundance of *Trichodesmium* spp. in the entire study area was
315 positively correlated with the nitrogen fixation rate at the surface ($r^2 = 0.80$; $p < 0.05$
316 [$r^2 = 0.52$; $p < 0.05$ if the datum taken at the *Trichodesmium*-bloom station T0906 is
317 excluded]) (Fig. 6c), suggesting that they significantly contributed to nitrogen fixation
318 in the study region. However, active nitrogen fixation occurred in the ECS where
319 *Trichodesmium* abundance was low, and hence, the other diazotrophs could also be
320 important for nitrogen fixation.

321

322 3.3. Observation around the Miyako Islands during the KT-09-17 cruise

323 The SST was lower to the northwest of the Miyako Islands than in adjacent

324 waters, and chl *a* was enriched in the same location (Fig. 4b,c). Therefore, the
325 enhanced productivity was probably due to nutrient supply by upwelling. This
326 upwelling generally occurs in the lee of islands (Hasegawa et al., 2009), suggesting
327 that there was a northward current during the cruise. The surface salinity was lower
328 east of the Miyako Islands than in the surrounding waters (Fig. 4a). The absence of
329 any large river on the east side of Miyako-jima Island and the separation of low
330 salinity water from the island suggest that the low salinity was caused by rainfall.

331 St. T0904 was located near the upwelling water; its SST of 29.0°C was lowest and its
332 surface N+N concentration of 374 nM was highest among all of the stations. However,
333 the N+N concentration at St. T0904 at the surface was higher than that at the
334 subsurface (an approximate depth of 50 m; Fig. S4), indicating that St. T0904 was not
335 located in the middle of the upwelling. At St. T0904, the surface phosphate
336 concentration was also highest (23 nM) and the N/P ratio (=16.3) was higher than the
337 Redfield ratio. With the exception of the surface at St. T0904, the phosphate
338 concentration was low (<3–9 nM) in the upper 50 m, with no noticeable variation
339 among the stations (Fig. 2a). The dissolved iron concentration varied between 0.19
340 and 0.89 nM at the surface (Fig. 2b). The highest dissolved iron concentration was
341 observed at St. T0907.

342 During the same cruise, we encountered a *Trichodesmium* spp. bloom at St.
343 T0906 (Fig. 2c), which had colored water at the surface. The abundance of
344 *Trichodesmium* spp. at St. T0906 was $>20,000$ filaments L^{-1} , which was far higher
345 than that at other stations (2–102 filament L^{-1}). The nitrogen fixation rate at the
346 surface ($61.9 \text{ nmol N } L^{-1} \text{ d}^{-1}$) of this station was more than 30-fold that just below the
347 surface, and was the highest among all of the stations (Fig. 3h). The diatom
348 abundance was markedly higher at St. T0904 than that at the other stations.
349 *Cylindrotheca closterium* was the most numerically dominant diatom (59%), followed
350 by *Navicula* spp. (23%) and *Nitzschia* spp. (13%). *C. closterium* was not detected at
351 the other stations, indicating that the high chl *a* induced by the island wake effect
352 mainly consisted of diatoms.

353

354 3.4. Numerical simulation

355 As the Kuroshio generally flows along the continental slope north of the Miyako
356 Islands (Fig. 1b), particles around the Miyako Islands were not transported along the
357 typical path of the Kuroshio to the northeast, especially at their initial stages (Fig. 7a).
358 Some particles migrated around the Miyako Islands, or turned south after they passed
359 the Tokara Strait. Nevertheless, the particles delivered to Area K east of the Tokara

360 Strait increased as time elapsed, and the ratio of particles delivered to Area K to the
361 total released particles ranged from 13–56% ($30 \pm 16\%$) by day 120 in 2003–2009
362 (Fig. 7b). The year-to-year variations in the ratio are mainly due to influences of
363 mesoscale eddies as partly seen in the particle trajectories in Fig. 7a, and likely
364 occurred over relatively short time scales (shorter than the seasonal time scale). This
365 is supported by another series of experiments in which particles were released on June
366 1, 11, and 21, and July 1 in 2009, which yielded ratios of 6.2–38% ($22 \pm 13\%$) by day
367 120 (Fig. S5).

368

369 **4. DISCUSSION**

370 **4.1. Distribution of phosphate and dissolved iron concentrations**

371 Phosphate concentrations were consistently low within the MLD in all of the
372 studied areas, and the maximum abundance of *Trichodesmium* spp. and total nitrogen
373 fixation activity generally occurred near the surface, suggesting that the phosphate
374 conditions for surface *Trichodesmium* spp. and other diazotrophs were similar among
375 all of the areas. Furthermore, with the exception of St. T1004 located near the
376 continental shelf, the vertical distribution of phosphate in the Kuroshio was analogous
377 to that in the Philippine Sea. Therefore, at least in the oceanic region of the two areas,

378 phosphate availability for *Trichodesmium* spp. and the other diazotrophs was similar
379 throughout the water column.

380 The surface distribution of the dissolved iron concentration demonstrated no
381 significant variation among the areas. The dissolved iron concentration (0.19–0.89
382 nM) was higher than that in the western North Pacific subtropical region (0.15–0.4
383 nM) (Brown et al., 2005). Obata et al. (1997) demonstrated that the vertical
384 distribution of the dissolved iron concentration in the ECS showed two peaks (at the
385 surface and in the deep water), suggesting that aerial dust significantly contributes to
386 the high dissolved iron concentration at the surface in all of our study areas. In
387 accordance with our results, previous modeling studies estimated the amount of dust
388 deposition to be similar in all four areas (Jickells et al., 2005; Mahowald et al., 2009).
389 Therefore, iron availability for *Trichodesmium* spp. and the other diazotrophs was also
390 likely similar across all of the study areas. Iron can be supplied from deep water to the
391 surface by mixing processes (Johnson et al., 1999). However, if this were the case, the
392 nitrate concentration would be expected to increase simultaneously at the surface
393 (Johnson et al., 1999), and we observed no noticeable elevation in N+N in any of the
394 areas, except at St. T0904. High concentrations of dissolved iron (>0.8 nM)
395 corresponded with low salinity at Sts. T0622 and T0907, suggesting that wet

396 deposition was an important process for iron supply. Dry deposition could also be
397 important since the iron-enriched water at Sts. T0601 and T0715 did not correspond
398 with low salinity.

399 Satellite data analysis indicated that there was a “pipeline” of material transport
400 from the Miyako Islands to the Kuroshio, and this was supported by numerical
401 simulations. According to the hypothesis of Marumo and Asaoka (1974), the growth
402 of *Trichodesmium* in the Kuroshio could be maintained by the supply of iron and
403 phosphorus from the islands situated along the Kuroshio, and the Miyako Islands
404 were considered a possible nutrient source to the Kuroshio. Hence, assuming this
405 hypothesis to be valid, the iron and phosphate concentrations near the Miyako Islands
406 (especially in our observed area) would be expected to be higher than those in the
407 other areas. However, we observed no significant difference in the iron and phosphate
408 concentrations among the four areas. This suggested that there was no detectable
409 washout of iron and phosphorus from the Miyako Islands during our observations, or
410 that diazotrophs and other phytoplankton exhausted the nutrient supply close to the
411 islands.

412

413 **4.2. Factors controlling the distributions of *Trichodesmium* spp. and**

414 **nitrogen fixation**

415 Although there was no statistically significant difference in *Trichodesmium* spp.
416 abundance among the study areas probably because the data were limited and the
417 variation was large, *Trichodesmium* spp. were always observed in the Kuroshio and
418 were abundant at most stations. Furthermore, at St.CK-10 in the East China Sea which
419 is in the Kuroshio branch current, a high abundance of *Trichodesmium* spp. was
420 observed. On the other hand, *Trichodesmium* spp. abundance in the Philippine Sea
421 tended to be lower than in the other areas. Such *Trichodesmium* distribution was also
422 reported in the previous study (Marumo and Asaoka, 1974). The present study also
423 showed lower surface nitrogen fixation in the Philippine Sea compared to that in the
424 Kuroshio ($p < 0.05$, *t*-test). Previous studies demonstrated that *Trichodesmium* spp.
425 flourished in some regions of the subtropical ocean where the iron levels were high
426 (Moore et al., 2009; Shiozaki et al., 2014b), which can be attributed to the high iron
427 requirement of *Trichodesmium* spp. for their growth compared to other diazotrophs
428 and non-diazotrophs (Kustka et al., 2003; Saito et al., 2011). Therefore, the
429 distribution of *Trichodesmium* spp. in the study area was expected to be associated
430 with the dissolved iron concentration at the surface. Furthermore, the iron-enhanced
431 active nitrogen fixation causes phosphorus depletion, and is consequently limited by

432 phosphorus (Mather et al., 2008). No significant differences in surface iron and
433 phosphate were observed among the study areas, which cannot explain the
434 distribution of *Trichodesmium* spp. and nitrogen fixation in the study region.

435 Johnson et al. (1999) reported that the iron supply increased around the
436 continental shelf because re-suspension from the bottom to the euphotic zone
437 becomes significant. However, in the continental shelf of the ECS, the abundance of
438 *Trichodesmium* spp. and nitrogen fixation were low (Marumo and Asaoka, 1974;
439 Zhang et al., 2012). Zhang et al. (2012) suggested that the low nitrogen fixation in the
440 continental shelf was attributable to mixing processes and the influence of the
441 Changjiang River. Turbulence near the sea floor influences the surface water in the
442 shallower bottom region (Matsuno et al., 2006), and Zhang et al. (2012) suggested
443 that the physical disturbance reduces diazotrophy since diazotrophs including
444 *Trichodesmium* favor calm seas. Furthermore, the water in the continental shelf of the
445 ECS is strongly influenced by the Changjiang River. The N/P ratio of the Changjiang
446 River plume is significantly higher than the Redfield ratio, which results in
447 phosphorus limitation, and can contribute to the low nitrogen fixation (Zhang et al.,
448 2012). In the present study, despite the fact that the surface phosphate concentration
449 was low throughout the study areas, the N/P ratio was generally lower than the

450 Redfield ratio, suggesting that biological production was limited by the availability of
451 nitrogen compared to phosphate (Moore et al., 2008, 2013). Furthermore, the
452 insignificant difference in MLD among the ECS, the Kuroshio, and the Philippine Sea
453 ($p>0.05$; Tukey HSD test) indicated similar vertical mixing conditions. Therefore, the
454 environmental variables related to nitrogen fixation only slightly differed as
455 demonstrated by the nMDS plot.

456 In our study, we found a *Trichodesmium* spp. bloom near the Miyako Islands.
457 Recent studies demonstrated that *Trichodesmium* spp. thrived near oceanic islands
458 (Shiozaki et al., 2010, 2014c; Dupouy et al., 2011). Given that some aspect of the
459 environment around the islands increases *Trichodesmium* spp. abundance and that
460 they are transported from the islands to the Kuroshio, this can explain why the
461 *Trichodesmium* distribution was not estimated from environmental variables.
462 Accordingly, the low abundance of *Trichodesmium* spp. in the Philippine Sea was
463 likely due to the low density of islands. Furthermore, higher nitrogen fixation in the
464 Kuroshio than in the Philippine Sea might be explained in the same manner.
465 *Trichodesmium* is a major nitrogen fixer in the Kuroshio (Chen et al., 2008, 2014;
466 Shiozaki et al., 2014a), and our results showed that the bulk water nitrogen fixation
467 was positively correlated with *Trichodesmium* abundance.

468 The numerical simulation demonstrated that released particles from the Miyako
469 Islands were generally transported to the northeast and flowed along the Kuroshio
470 during summer between 2003 and 2009. Thus, if *Trichodesmium* increases and active
471 nitrogen fixation usually occurs around the Miyako Islands, the water would be
472 delivered to the Kuroshio. Furthermore, we performed additional particle tracking
473 experiments whose particle release points were set at major islands in the Ryukyu
474 Islands (Amami Islands, Okinawa Main Island, and the Ishigaki Islands) (Figs. S6 and
475 S7). The results demonstrated that the particles released from the other islands of the
476 Miyako Islands were also delivered to the Kuroshio, with some exceptions. Based on
477 the calculations for 2003–2009, 13–56% ($30 \pm 16\%$) of particles released from the
478 islands reached Area K by day 120 (Fig. S7).

479 Studies on nitrogen fixation around islands in the study region are fairly limited
480 (Liu et al., 2013), and the present study is the first report of a *Trichodesmium* bloom
481 around islands in the area. The Miyako Islands are surrounded by reefs, and studies
482 have shown that *Trichodesmium* blooms can be associated with reef environments
483 (Bell et al., 1999; McKinna et al., 2011). However, the factors causing the
484 *Trichodesmium* blooms around islands are not well understood (Shiozaki et al.,
485 2014c). Further studies are required to identify which characteristics of the near island

486 environment are important for the growth and/or accumulation of *Trichodesmium* and
487 other diazotrophs.

488

489 5. CONCLUSIONS

490 We hypothesize that the high abundance of *Trichodesmium* spp. and active
491 nitrogen fixation in the Kuroshio were ascribable not to the unique nutrient
492 environment, but rather to the supply of *Trichodesmium* spp. and other diazotrophs
493 from the surrounding islands. The Ryukyu Islands would not be the only islands with
494 abundant *Trichodesmium* spp., as *Trichodesmium* spp. also flourish in the upstream
495 Kuroshio near Luzon Island (Chen et al., 2008). Therefore, the abundance of
496 *Trichodesmium* spp. would be generally increased around islands situated along the
497 Kuroshio, and the abundant *Trichodesmium* spp. would likely be transported to the
498 mainstream of the Kuroshio. *Trichodesmium* is a major diazotroph in the Kuroshio
499 (Chen et al., 2008, 2014; Shiozaki et al., 2014a), and diazotrophy in the Kuroshio is
500 considered to influence the nutrient stoichiometry in the North Pacific (Shiozaki et al.,
501 2010). Thus, our results indicate that phenomena around the islands located along the
502 Kuroshio are important for determining the partial nitrogen inventory in the North
503 Pacific.

504

505 **Author Contributions**

506 T.S., S.T., S.I., and K.F. designed the experiment and T.S., S.T., T.K., X.L., F.H., and
507 K.F. collected the samples at sea. T.S. determined nitrogen fixation and abundance of
508 *Trichodesmium* spp. during the KT-06-21, KT-07-21, KT-09-17, and *Nagasaki-maru*
509 242 cruises, and X.L. did during the KT-10-19 cruise. T.S. analyzed datasets of
510 satellite and climatological current field. S.T. analyzed concentration of dissolved iron.
511 S.I. performed numerical experiments. T.K. and F.H. determined nutrient
512 concentration. T.S. prepared the manuscript with contributions from all co-authors.

513

514 **Acknowledgements**

515 We thank J. Ishizaka, the captains, crew members, and participants on board the
516 T/V *Nagasaki-maru* and R/V *Tansei-maru* cruises for their cooperation at sea.
517 Thanks also to K. Hayashizaki for his support in use of the mass spectrometer at
518 Kitasato University, to A. Takeshige and J. Hirai for their valuable comments on
519 biology in the Kuroshio, and to T. Kitahashi for his suggestion on statistical analyses.
520 Comments from two anonymous reviewers greatly improved the paper. We appreciate
521 NASA ocean color processing group for providing the chl *a* data set and Japan
522 Oceanographic Data Center for ADCP data set. This research was financially

523 supported by MEXT grant on Priority Areas (18067006 & 21014006) and by
524 Innovative Areas (24121001, 24121005, & 24121006) and by Grant-in-Aid for JSPS
525 Fellows (25-7341).
526

527 **References**

- 528 Bell, P.R.F., Elmetri, I., Uwins, P.: Nitrogen fixation by *Trichodesmium* spp. in the
529 central and northern Great Barrier Reef lagoon: relative importance of the
530 fixed-nitrogen load, Mar. Ecol. Progr. Ser., 186, 119-126, 1999.
- 531 Brown, M.T., Landing, W.M., Measures, C.I.: Dissolved and particulate Fe in the
532 western and central North Pacific: Results from the 2002 IOC cruise, Geochem.
533 Geophys. Geosyst., 6(10), Q10001, 2005.
- 534 Capone, D.G., Zehr, P.J., Paerl, H.W., Bergman, B., Carpenter, E.J.: *Trichodesmium*,
535 a globally significant marine cyanobacterium, Science, 276, 1221-1229, 1997.
- 536 Chen, C.T.A.: Distributions of nutrients in the East China Sea and the South China
537 Sea connection, J. Oceanogr., 64, 737-751, 2008.
- 538 Chen, Y.L.L., Chen, H.Y., Tuo, S.H., Ohki, K.: Seasonal dynamics of new production
539 from *Trichodesmium* N₂ fixation and nitrate uptake in the upstream Kuroshio and
540 South China Sea basin, Limnol. Oceanogr., 53(5), 1705-1721, 2008.
- 541 Chen, Y.L.L., Chen, H.Y., Lin, Y.H., Yong, T.C., Taniuchi, Y., Tuo, S.H.: The
542 relative contributions of unicellular and filamentous diazotrophs to N₂ fixation in the
543 South China Sea and the upstream Kuroshio, Deep-Sea Res. I, 85, 56-71, 2014.
- 544 Dabundo, R., Lehmann, M.F., Treibergs, L., Tobias, C.R., Altabet, M.A.: The

545 contamination of commercial $^{15}\text{N}_2$ gas stocks with ^{15}N -labeled nitrate and ammonium
546 and consequences for nitrogen fixation measurements, PLoS one, 9(10), e110335,
547 2014.

548 Dupouy, C., Benielli-Gary, D., Neveux, J., Dandonneau, Y., Westberry, T.K.: An
549 algorithm for detecting *Trichodesmium* surface blooms in the South Western Tropical
550 Pacific, Biogeosciences, 8, 3631-3647, 2011.

551 Großkopf, T., Mohr, W., Baustian, T., Schunck, H., Gill, D., Kuypers, M.M.M., Lavik,
552 G., Schmitz, R.A., Wallace, D.W.R., LaRoche, J.: Doubling of marine
553 dinitrogen-fixation rate based on direct measurements, Nature, 488, 361-364, 2012.

554 Hasegawa, D., Lewis, M.R., Gangopadhyay, A.: How islands cause phytoplankton to
555 bloom in their wake, Geophys. Res. Lett., 36, L20605, 2009.

556 Hashihama, F., Furuya, K., Kitajima, S., Takeda, S., Takemura, T., Kanda, J.:
557 Macro-scale exhaustion of surface phosphate by dinitrogen fixation in the western
558 North Pacific, Geophys. Res. Lett., 36, L03610, 2009.

559 Isobe, A.: Recent advances in ocean-circulation research on the Yellow Sea and East
560 China Sea shelves, J. Oceanogr., 64, 569-584, 2008.

561 Itoh, S., Yasuda, I., Nishikawa, H., Sasaki, H., Sasai, Y.: Transport and environmental
562 temperature variability of eggs and larvae of the Japanese anchovy (*Engraulis*

563 *japonicus*) and Japanese sardine (*Sardinops melanostictus*) in the western North
564 Pacific estimated via numerical particle-tracking experiments, *Fish. Oceanogr.*, 18(2),
565 118-133, 2009.

566 Jickells, T.D., An, Z.S., Andersen, K.K., Baker, A.R., Bergametti, G., Brooks, N.,
567 Cao, J.J., Boyd, P.W., Duce, R.A., Hunter, K.A., Kawahata, H., Kubilay, N., LaRoche,
568 J., Liss, P.S., Mahowald, N., Prospero, J.M., Ridgwell, A.J., Tegen, I., Torres, R.:
569 Global iron connections between desert dust, ocean biogeochemistry, and climate,
570 *Science*, 308, 67-71, 2005.

571 Johnson, K.S., Chavez, F.P., Friederich, G.E.: Continental-shelf sediment as a
572 primary source of iron for coastal phytoplankton, *Nature*, 398, 697-700, 1999.

573 Johnson, K.S., Boyle, E., Bruland, K., Coale, K., Measures, C., Moffett, J.,
574 Aguilar-Islas, A., Barbeau, K., Bergquist, B., Bowie, A., Buck, K., Cai, Y., Chase, Z.,
575 Cullen, J., Doi, T., Elrod, V., Fitzwater, S., Gordon, M., King, A., Laan, P.,
576 Laglera-Baquer, L., Landing, W., Lohan, M., Mendez, J., Milne, A., Obata, H.,
577 Ossiander, L., Plant, J., Sarthou, G., Sedwick, P., Smith, G.J., Sohst, B., Tanner, S.,
578 Van den Berg, S., Wu, J.: The SAFe iron intercomparison cruise: an international
579 collaboration to develop dissolved iron in seawater standards, *Eos*, 88, 131-132, 2007.

580 Kodama, T., Furuya, K., Hashihama, F., Takeda, S., Kanda, J.: Occurrence of

581 rain-origin nitrate patches at the nutrient-depleted surface in the East China Sea and
582 the Philippine Sea during summer, *J. Geophys. Res.*, 116, C08003, 2011.

583 Kustka, A., Sañudo-Wilhelmy, S., Carpenter, E.J., Capone, D.G., Raven, J.A.: A
584 revised estimate of the iron use efficiency of nitrogen fixation, with special reference
585 to the marine cyanobacterium *Trichodesmium* spp. (Cyanophyta), *J. Phycol.*, 39,
586 12-25, 2003.

587 Lin, I.-I., Hu, C., Li, Y.-H., Ho, T.-Y., Fischer, T.P., Wong, G.T.F., Wu, J., Huang,
588 C.-W., Chu, D.A., Ko, D.S., Chen, J.-P. : Fertilization potential of volcanic dust in the
589 low-nutrient low-chlorophyll western North Pacific subtropical gyre: Satellite
590 evidence and laboratory study, *Glob. Biogeochem. Cycles*, 25, GB1006,
591 doi:10.1029/2009GB003758, 2011.

592 Liu, X., Furuya, K., Shiozaki, T., Masuda, T., Kodama, T., Sato, M., Kaneko, H.,
593 Nagasawa, M., Yasuda, I.: Variability in nitrogen sources for new production in the
594 vicinity of the shelf edge of the East China Sea in summer, *Cont. Shelf Res.*, 61-62,
595 23-30, 2013.

596 McKinna, L.I.W., Furnas, M.J., Ridd, P.V.: A simple, binary classification algorithm
597 for detection of *Trichodesmium* spp. within the Great Barrier Reef using MODIS
598 imagery, *Limnol. Oceanogr.; Methods*, 9, 50-66, 2011.

599 Mahaffey, C., Michaels, A.F., Capone, D.G.: The conundrum of marine N₂ fixation,
600 Am. J. Sci., 305, 546-595, 2005.

601 Mahowald, N.M., Engelstaedter, S., Luo, C., Sealy, A., Artaxo, P., Benitez-Nelson, C.,
602 Bonnet, S., Chen, Y., Chuang, P.Y., Cohen, D.D., Dulac, F., Herut, B., Johansen,
603 A.M., Kubilay, N., Losno, R., Maenhaut, W., Paytan, A., Prospero, J.M., Shank, L.M.,
604 Siefert, R.L.: Atmospheric iron deposition: Global distribution, variability, and human
605 perturbations, Annu. Rev. Mar. Sci., 1, 245-278, 2009.

606 Marumo, R., Asaoka, O.: *Trichodesmium* in the East China Sea 1. Distribution of
607 *Trichodesmium thiebautii* GOMONT during 1961-1967, J. Oceanogr. Soc. Japan, 30,
608 298-303, 1974.

609 Mather, R.L., Reynolds, S.E., Wolff, G.A., Williams, R.G., Torres-Valdes, S.,
610 Woodward, E.M.S., Landolfi, A., Pan, X., Sanders, R., Achterberg, E.P.: Phosphorus
611 cycling in the North and South Atlantic Ocean subtropical gyres, Nat. Geosci., 1,
612 439-443, 2008.

613 Matsuno, T., Lee, J.S., Shimizu, M., Kim, S.H., Pang, I.C.: Measurements of the
614 turbulent energy dissipation rate ϵ and an evaluation of the dispersion process of the
615 Changjiang Diluted Water in the East China Sea, J. Geophys. Res., 111, C11S09,
616 2006.

617 McGowan, J.A.: Oceanic biogeography of the Pacific, in: The micropaleontology of
618 the oceans, Cambridge University Press, Cambridge, 3-74, 1971.

619 Miyazawa, Y., Zhang, R., Guo, X., Tamura, H., Ambe, D., Lee, J.S., Okuno, A.,
620 Yoshinari, H., Setou, T., Komatsu, K.: Water mass variability in the western North
621 Pacific detected in a 15-year eddy resolving ocean reanalysis, *J. Oceanogr.*, 65,
622 737-756, 2009.

623 Mohr, W., Großkopf, T., Wallace, D.W.R., LaRoche, J.: Methodological
624 underestimation of oceanic nitrogen fixation rate, *PLoS one*, 5(9), e12583, 2010.

625 Montoya, J.P., Voss, M., Kähler, P., Capone, D.G.: A simple, high-precision,
626 high-sensitivity tracer assay for N₂ fixation, *Appl. Environ. Microbiol.*, 62(3),
627 986-993, 1996.

628 Moore, C.M., Mills, M.M., Langlois, R., Milne, A., Achterberg, E.P., LaRoche, J.,
629 Geider, R.J.: Relative influence of nitrogen and phosphorus availability on
630 phytoplankton physiology and productivity in the oligotrophic sub-tropical North
631 Atlantic Ocean, *Limnol. Oceanogr.*, 53(1), 291-305, 2008.

632 Moore, C.M., Mills, M.M., Achterberg, E.P., Geider, R.J., LaRoche, J., Lucas, M.I.,
633 McDonagh, E.L., Pan, X., Poulton, A.J., Rijkenberg, M.J.A., Suggett, D.J., Ussher,
634 S.J., Woodward, E.M.S.: Large-scale distribution of Atlantic nitrogen fixation

635 controlled by iron availability, *Nat. Geosci.*, 2, 867-871, 2009.

636 Moore, C.M., Mills, M.M., Arrigo, K.R., Berman-Frank, I., Bopp, L., Boyd, P.W.,
637 Galbraith, E.D., Geider, R.J., Guieu, C., Jaccard, S.L., Jickells, T.D., LaRoche, J.,
638 Lenton, T.M., Mahowald, N.M., Marañón, E., Marinov, I., Moore, J.K., Nakatsuka, T.,
639 Oschlies, A., Saito, M.A., Thingstad, T.F., Tsuda, A., Ulloa, O.: Processes and
640 patterns of oceanic nutrient limitation, *Nat. Geosci.*, 6, 701-710, 2013.

641 Obata, H., Karatani, H., Nakayama, E.: Automated determination of iron in seawater
642 by chelating resin concentration and chemiluminescence detection, *Anal. Chem.*, 65,
643 1524-1528, 1993.

644 Obata, H., Karatani, H., Matsui, M., Nakayama, E.: Fundamental studies for chemical
645 speciation of iron in seawater with an improved analytical method, *Mar. Chem.*, 56,
646 97-106, 1997.

647 Saito, M.A., Bertrand, E.M., Dutkiewicz, S., Bulygin, V.V., Moran, D.M., Monteiro,
648 F.M., Follows, M.J., Valois, F.W., Waterbury, J.B.: Iron conservation by reduction of
649 metalloenzyme inventories in the marine diazotroph *Crocospaera watsonii*, *Proc.*
650 *Natl. Acad. Sci. USA*, 108, 2184-2189, 2011.

651 Shiozaki, T., Furuya, K., Kodama, T., Takeda, S.: Contribution of N₂ fixation to new
652 production in the western North Pacific Ocean along 155°E, *Mar. Ecol. Progr. Ser.*,

653 377, 19-32, 2009.

654 Shiozaki, T., Furuya, K., Kodama, T., Kitajima, S., Takeda, S., Takemura, T., Kanda,
655 J.: New estimation of N₂ fixation in the western and central Pacific Ocean and its
656 marginal seas., *Glob. Biogeochem. Cycles*, 24, GB1015, 2010.

657 Shiozaki, T., Furuya, K., Kurotori, H., Kodama, T., Takeda, S., Endoh, T., Yoshikawa,
658 Y., Ishizaka, J., Matsuno, T.: Imbalance between vertical nitrate flux and nitrate
659 assimilation on a continental shelf: Implications of nitrification, *J. Geophys. Res.*, 116,
660 C10031, 2011.

661 Shiozaki, T., Chen, Y.L.L., Lin, Y.H., Taniuchi, Y., Sheu, D.S., Furuya, K., Chen,
662 H.Y.: Seasonal variations of unicellular diazotroph groups A and B, and
663 *Trichodesmium* in the northern South China Sea and neighboring upstream Kuroshio
664 Current, *Cont. Shelf Res.*, 80, 20-31, 2014a.

665 Shiozaki, T., Ijichi, M., Kodama, T., Takeda, S., Furuya, K.: Heterotrophic bacteria as
666 major nitrogen fixers in the euphotic zone of the Indian Ocean, *Glob. Biogeochem.*
667 *Cycles*, 28, 1096-1110, 2014b.

668 Shiozaki, T., Kodama, T., Furuya, K.: Large-scale impact of the island mass effect
669 through nitrogen fixation in the western South Pacific Ocean, *Geophys. Res. Lett.*, 41,
670 2907-2913, 2014c.

671 Wilson, C., Qiu, X.: Global distribution of summer chlorophyll blooms in the
672 oligotrophic gyres, *Progr. Oceanogr.*, 78, 107-134, 2008.

673 Zhang, R., Chen, M., Cao, J., Ma, Q., Yang, J., Qiu, Y.: Nitrogen fixation in the East
674 China Sea and southern Yellow Sea during summer 2006, *Mar. Ecol. Progr. Ser.*, 447,

675 77-86, 2012.

676

677 Table 1 Summary of *Trichodesmium* at the surface, and depth-integrated nitrogen

678 fixation and its related parameters in the four representative study areas.

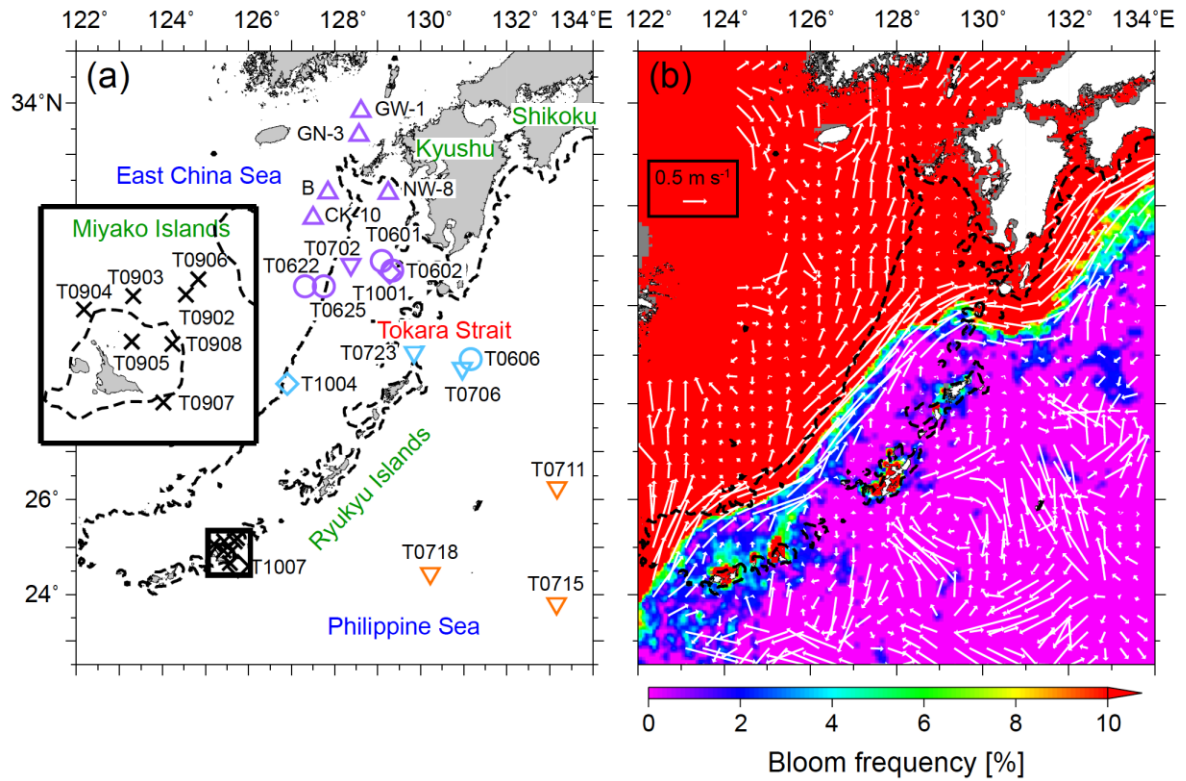
Area	<i>Trichodesmium</i> * [filaments l ⁻¹]	N ₂ fixation [μmolN L ⁻¹ d ⁻¹]	Temperature* [°C]	MLD [m]	NO ₃ ⁻ +NO ₂ ^{-*} † [nM]	PO ₄ ^{3-*} † [nM]	DFe* [nM]
East China Sea	21±58	170±140	28.5±1.2	24±12	19±11	15±9	0.76±0.18
Kuroshio	43±33	199±142	29.4±0.81	27±8	9±8	15±7	0.45±0.13
Philippine Sea	8±8	58.3±25.1	29.4±0.1	23±3	8±3	14±19	0.51±0.25
Miyako Islands	3019±8478	201±274	29.3±0.3	40±12	61±128	8±7	0.38±0.24

679 * values in surface water

680 †When the concentration was below the detection limit (3 nM), we assumed a concentration of 3 nM to

681 calculate the mean.

682



683

684

685 Figure 1. (a) Sampling stations during the KT-06-21 (circles), KT-07-22 (inverted

686 triangles), KT-09-17 (crosses), KT-10-19 (diamonds), and 242 (triangles) cruises.

687 Symbols of stations located in the East China Sea, the Kuroshio, the Philippine Sea,

688 and near the Miyako Islands are indicated in purple, light blue, orange, and black,

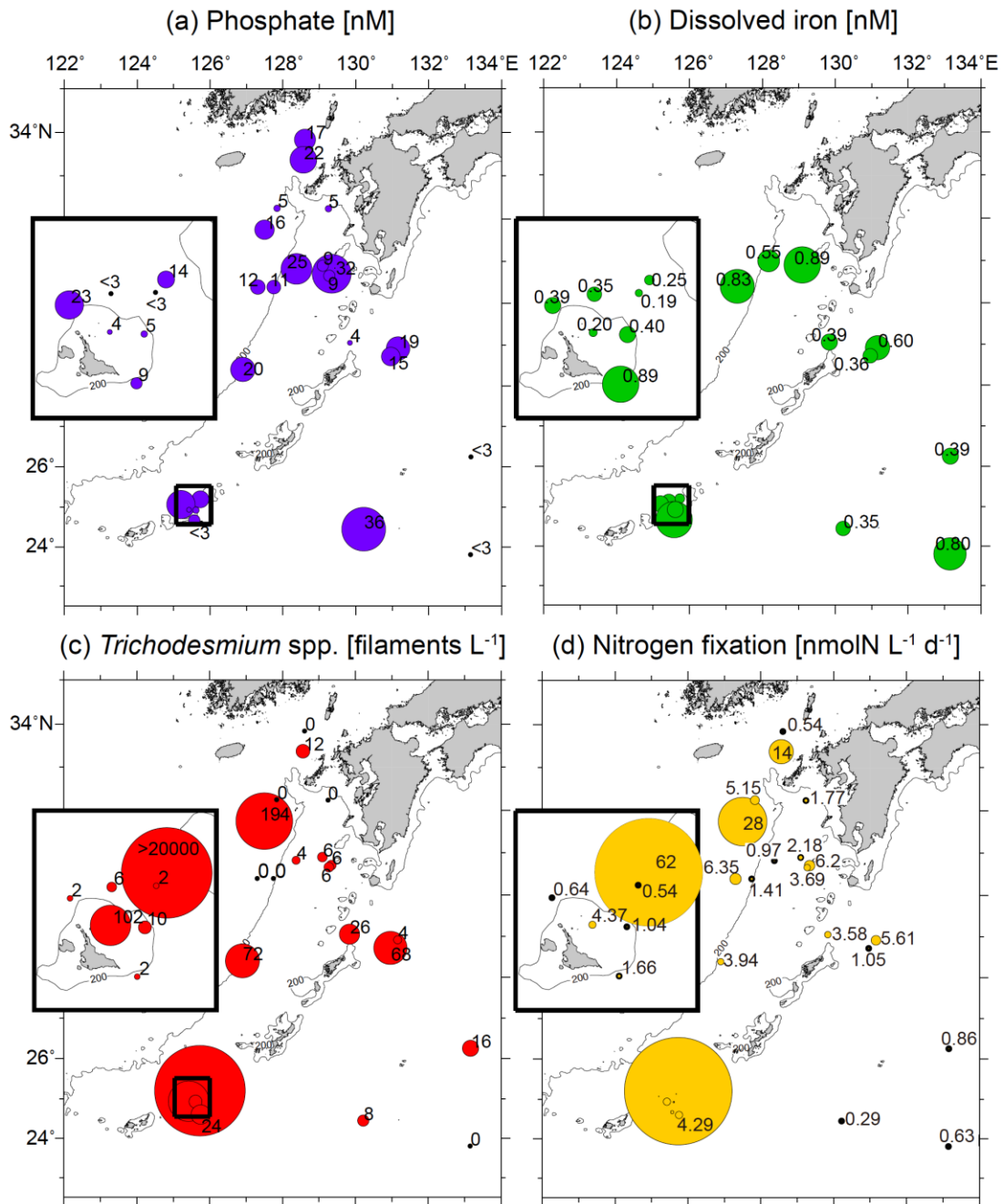
689 respectively. (b) Climatological surface current fields during summer (1953–2008)

690 from geoelectrokinetograph measurements and ship-mounted ADCP data. The

691 background contour represents the percentage of chlorophyll *a* of $>0.15 \text{ mg m}^{-3}$

692 during summer between 2003 and 2009. Dashed lines indicate 200 m isobaths.

693



694

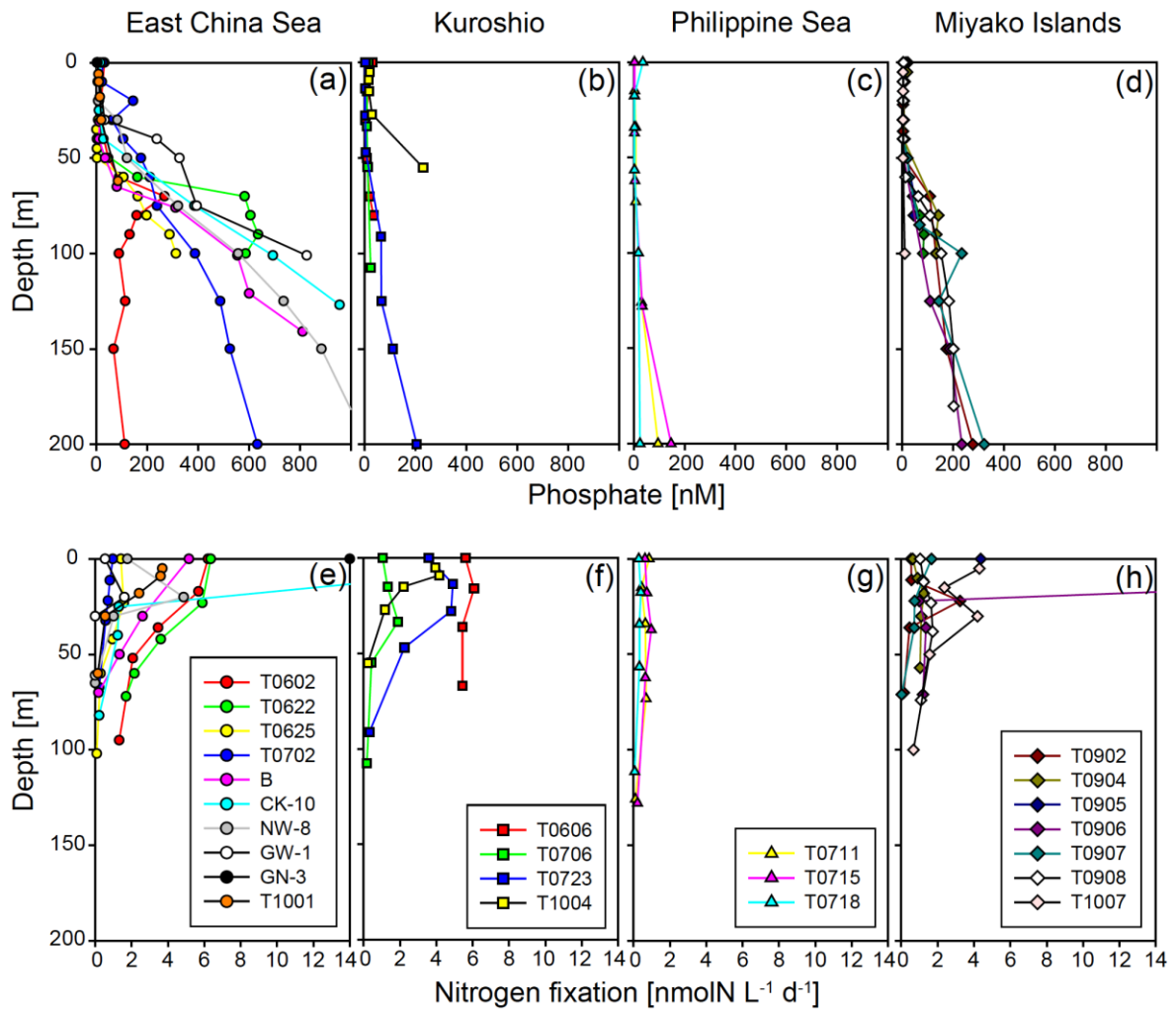
695

696 Figure 2. Distribution of (a) phosphate, (b) dissolved iron, (c) *Trichodesmium* spp.,

697 and (d) nitrogen fixation at the surface. The parameters in the small boxes indicate

698 results from the KT-09-17 cruise. The areas of the circles are proportional to the

699 concentration, abundance, or activity.



700

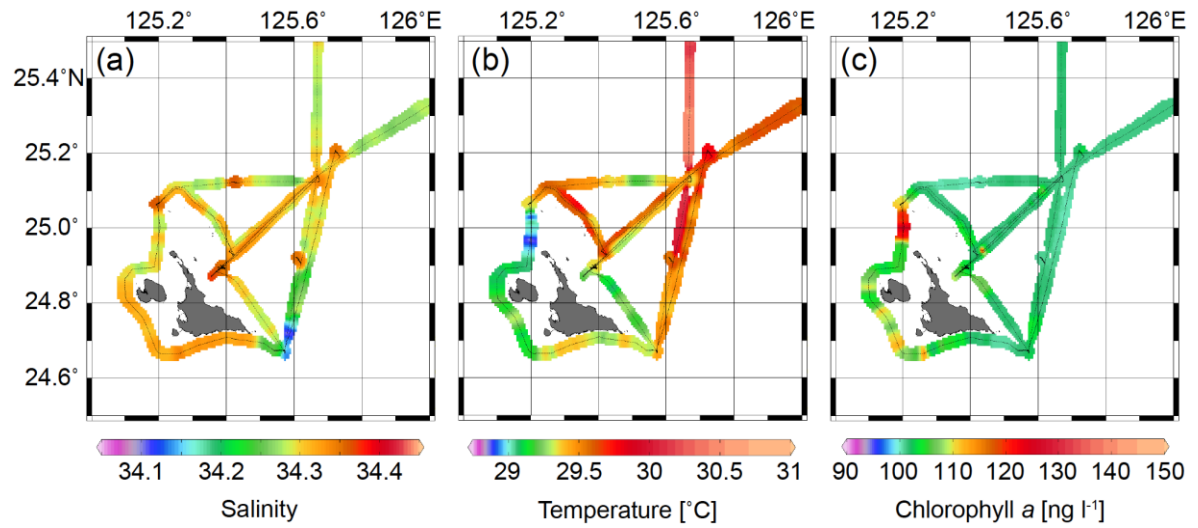
701

702 Figure 3. Vertical profiles of phosphate and nitrogen fixation in the East China Sea (a

703 and e), the Kuroshio (b and f), the Philippine Sea (c and g), and the Miyako Islands (d

704 and h).

705



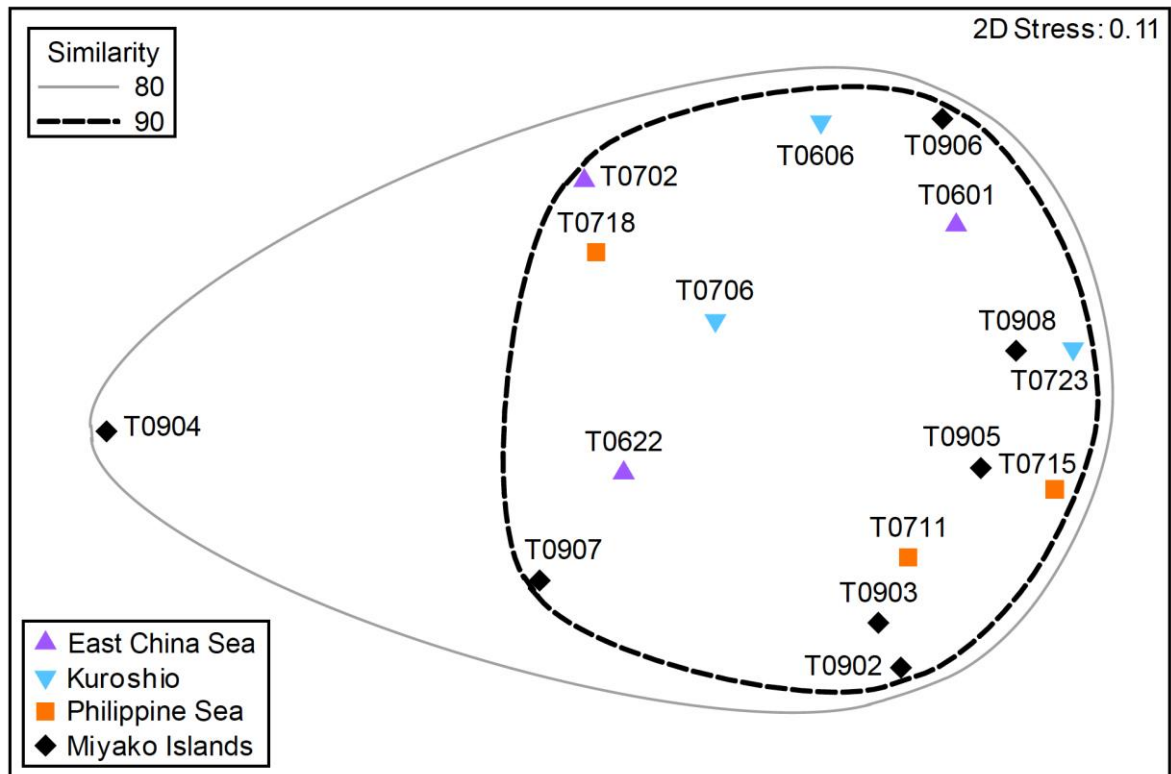
706

707

708 Figure 4. Surface (a) salinity, (b) temperature, and (c) chlorophyll *a* during the

709 KT-09-17 cruise.

710

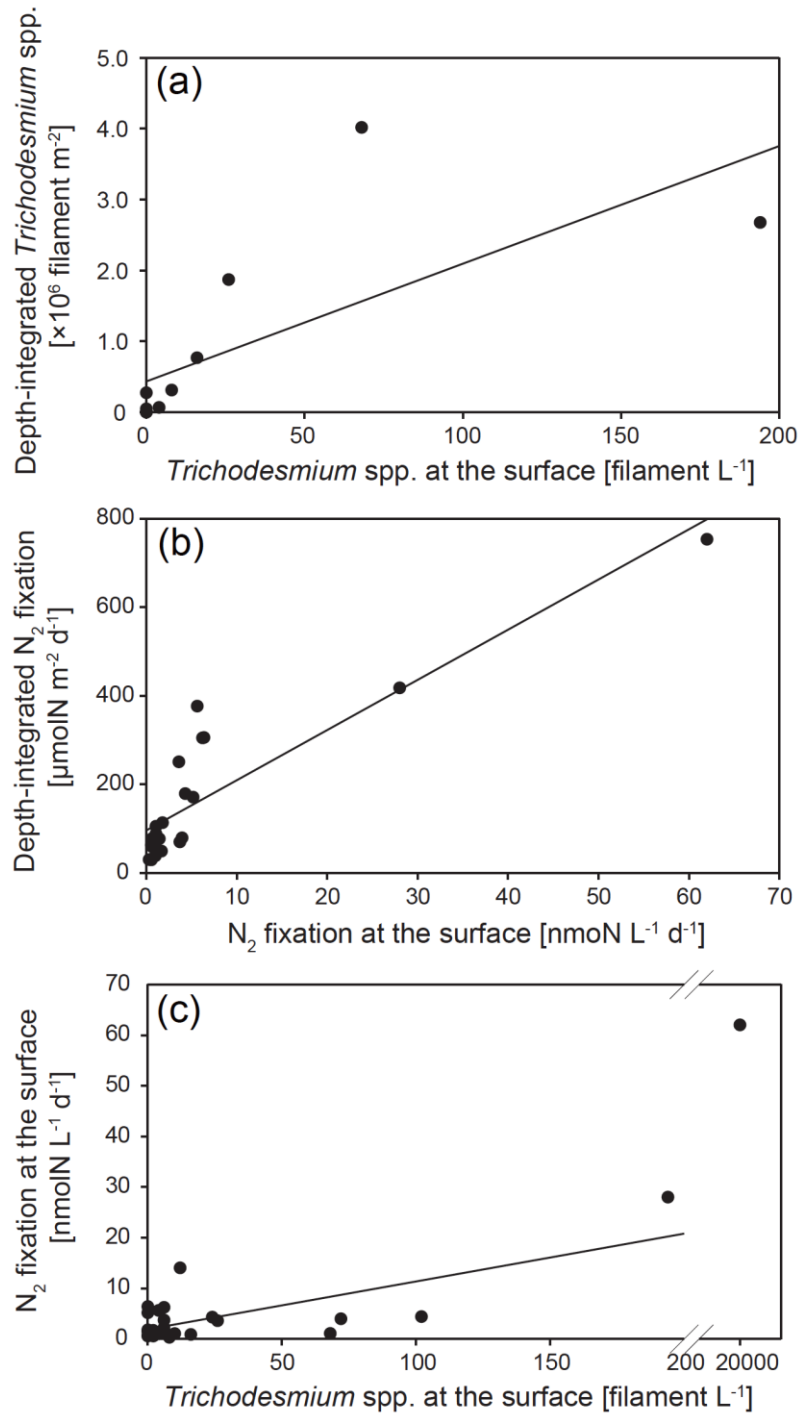


711

712

713 Figure 5. nMDS ordination of sampling stations with environmental variables

714



715

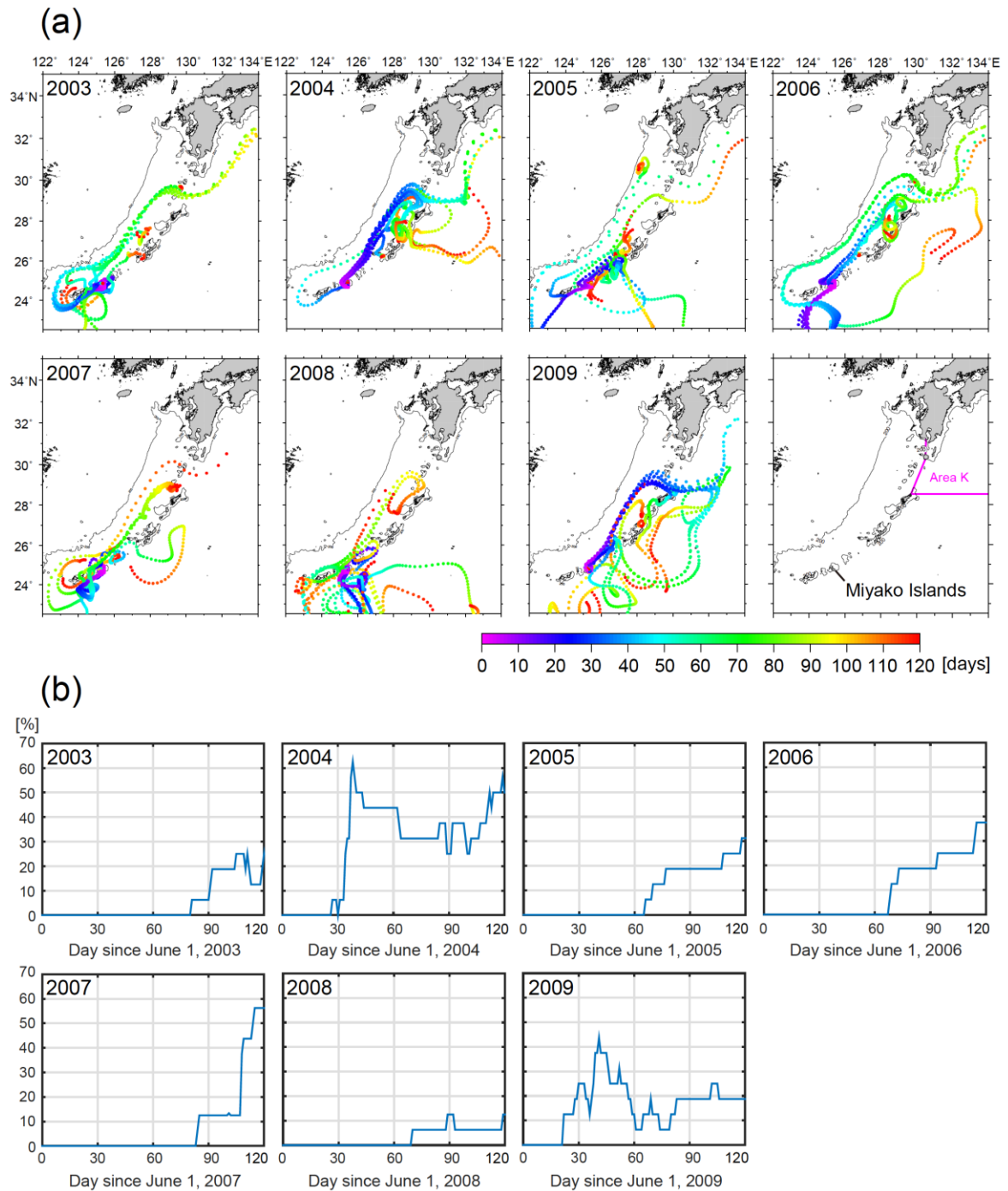
716

717 Figure 6. Relationships (a) between surface and depth-integrated *Trichodesmium* spp.

718 abundance, (b) between surface and depth-integrated nitrogen fixation rates, and (c)

719 between *Trichodesmium* spp. abundance and nitrogen fixation rate at the surface.

720



721

722

723 Figure 7. (a) Trajectories of particles released from points around the Miyako Islands

724 on June 1, 2003–2009. (b) The ratio of particles delivered to Area K to the total

725 released particles.